

Effects of errors in the solar radius on helioseismic inferences

Sarbani Basu

School of Natural Sciences, Institute for Advanced Study, Olden Lane, Princeton NJ 08540, U.S.A.

Accepted . Received

ABSTRACT

Frequencies of intermediate-degree f-modes of the Sun seem to indicate that the solar radius is smaller than what is normally used in constructing solar models. We investigate the possible consequences of an error in radius on results for solar structure obtained using helioseismic inversions. It is shown that solar sound speed will be overestimated if oscillation frequencies are inverted using reference models with a larger radius. Using solar models with radius of 695.78 Mm and new data sets, the base of the solar convection zone is estimated to be at radial distance of 0.7135 ± 0.0005 of the solar radius. The helium abundance in the convection zone as determined using models with OPAL equation of state is 0.248 ± 0.001 , where the errors reflect the estimated systematic errors in the calculation, the statistical errors being much smaller. Assuming that the OPAL opacities used in the construction of the solar models are correct, the surface Z/X is estimated to be 0.0245 ± 0.0006 .

Key words: Sun: oscillations — Sun: interior — Sun: abundances — Sun: convection

1 INTRODUCTION

Helioseismology has proved to be a remarkable tool that can be used to study the solar interior. Helioseismic inversion techniques have been used to probe details of the solar structure (cf., Gough et al. 1996; Basu et al. 1996; Kosovichev et al. 1997), abundances (cf., Basu & Antia 1995; Kosovichev 1996; Antia & Chitre 1997a), and rotation rate (cf., Thompson et al. 1996). Most inversions done so far assume that the radius of the Sun is known precisely and the value used is 695.99 Mm (Allen 1976).

Recent data from the Global Oscillation Network Group (GONG), and from the SOI/MDI instrument on board the SOHO spacecraft, allow the determination of the intermediate-degree solar f-mode frequencies very precisely. It has been shown by Antia (1997) and Schou et al. (1997) that the ratio of the newly determined solar f-mode frequencies and frequencies of the f-modes of standard solar models is very nearly a constant which differs significantly from unity. Since the f-mode frequencies are largely insensitive to the detailed structure of the Sun and depend mainly on the global parameters, the simplest explanation of this difference is that the radius assumed for the models is not the radius of the Sun. Antia (1997) estimated the solar radius to be 695.78 Mm using the GONG data, while Schou et al. (1997) using MDI data show that the apparent photospheric solar radius (695.99 Mm) used to calibrate the models should be reduced by approximately 0.3 Mm. This difference between the radius of the Sun and of solar models used as reference models for helioseismic inversions can lead to errors in our

estimation of the solar structure.

The exact value of the solar radius as determined by the f-modes depends to some extent on the surface physics used in the models (cf., Antia & Chitre 1997b). Although the frequencies of solar f-modes are remarkably insensitive to the structure of the solar interior, they do depend to a small extent on the details of the surface layers. The modes are affected particularly by the formulation used to calculate the convective flux and atmospheric opacities. Models constructed with the Canuto-Mazzitelli (1991) formulation for calculating the convective flux show that a smaller reduction in radius is needed for the model and observed f-mode frequencies to match, compared with the reduction needed for models constructed with the mixing length formalism. This difference is most probably responsible for the apparent difference of results found by Schou et al. (1997) using the data from the SOI/MDI instrument on board the SOHO spacecraft, and by Antia (1997) using data from GONG. As a result, there is still some uncertainty in the estimate of solar radius. However, if models with the same physics are used, then the GONG and MDI data give very similar results (Antia & Chitre 1997b).

An inversion for solar structure (e.g., Dziembowski, Pamyatnykh & Sienkiewicz 1990; Däppen et al. 1991; Antia & Basu 1994a; Dziembowski et al. 1994) generally proceeds through a linearisation of the equations of stellar oscillations around a known reference model. The differences between the structure of the Sun and the reference model are then related to the differences in the frequencies of the Sun and the model by kernels. Non-adiabatic effects and other er-

arXiv:astro-ph/9712133v1 9 Dec 1997

rors in modelling the surface layers give rise to frequency shifts (Cox & Kidman 1984; Balmforth 1992) which are not accounted for by the variational principle. In the absence of any reliable formulation, these effects have been taken into account in an *ad hoc* manner by including an arbitrary function of frequency in the variational formulation (Dziembowski et al. 1990). Thus the fractional change in frequency of a mode can be expressed in terms of fractional changes in the structure of the model and a surface term.

When the oscillation equation is linearised — under the assumption of hydrostatic equilibrium — the fractional change in the frequency can be related to the fractional changes in two of the functions that define the structure of the models. Thus,

$$\frac{\delta\omega_i}{\omega_i} = \int K_{1,2}^i(r) \frac{\delta f_1(r)}{f_1(r)} dr + \int K_{2,1}^i(r) \frac{\delta f_2(r)}{f_2(r)} dr + \frac{F_{\text{surf}}(\omega_i)}{E_i} \quad (1)$$

(cf., Dziembowski et al. 1990). Here $\delta\omega_i$ is the difference in the frequency ω_i of the i th mode between the solar data and a reference model. The functions f_1 and f_2 are an appropriate pair of functions like sound speed and density, or density and adiabatic index Γ_1 etc. The kernels $K_{1,2}^i$ and $K_{2,1}^i$ are known functions of the reference model which relate the changes in frequency to the changes in f_1 and f_2 respectively; and E_i is the inertia of the mode, normalized by the photospheric amplitude of the displacement. The term F_{surf} results from the near-surface errors.

The kernels $K_{1,2}^i$ and $K_{2,1}^i$ are normally calculated assuming that there is no difference between the radius of the Sun and the reference model (see Antia & Basu (1994a) for the steps involved in calculating the kernels for the pair (c^2, ρ)). Thus inversions of Eq. (1) are likely to introduce systematic errors if the radius of the reference model is different from that of the Sun or test model. This can be seen in Fig. 1 for inversion between two models. Hence, our results on solar sound speed are also likely to be modified if the radius of the solar model is different from that of the Sun, and initial results suggest that this is indeed the case (Antia 1997).

In this work we show how a mismatch of radius affects solar sound-speed results. Further, since most of our knowledge of the solar interior, e.g., depth of the convection zone (CZ), overshoot below the solar convection zone, helium abundance in the solar envelope, etc., are derived from the sound speed, we re-calibrate these quantities in view of possible changes in the value of solar radius. While determining the helium abundance we have looked into different sources of systematic errors, like opacities and depth of CZ, which had not been adequately examined in earlier studies. We also attempt to put limits on the heavy-element abundance in the solar envelope. Unlike most previous works which utilized oscillation data from the Big Bear Solar Observatory, in this work more precise data from GONG and SOI/MDI have also been used to determine the depth of the solar convection zone and the helium abundance.

The rest of the paper is organized as follows. In Section 2, we discuss the change in deduced sound-speed and density profiles in the Sun that results from using models that correspond to the reduced radius as determined from the

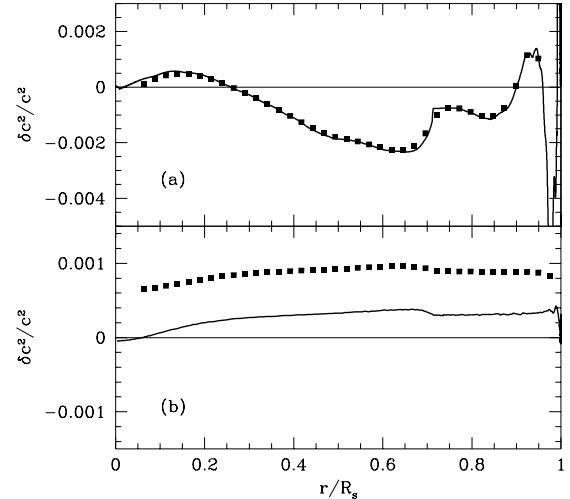


Fig. 1 The result of sound-speed inversions between different models. The continuous line is the exact sound-speed difference between the two models, the points are the results obtained by inverting the frequency differences between the two models. In Panel (a), both the reference and test models have the same radius, 695.99Mm, the difference between the two models is the equation of state used. In Panel (b), the models have identical input physics, but radii of the two models are different. The reference model has a radius of 695.99 Mm while the test model has a radius of 695.78 Mm.

f-mode frequencies. In Sections 3 and 4 we discuss the effect of the radius change on the deduced depth of the solar convection zone and helium abundance respectively. In Section 5 we try to investigate if an error in equation of state can explain the remaining difference between the sound speed of the Sun and solar models inside the convection zone. We present the conclusions from this study in Section 6.

2 INVERSION RESULTS

In this work we have used the subtractive optimally localized averages (SOLA) method of Pijpers & Thompson (1992) to invert Eq. (1). The procedure as applied to determine the sound-speed difference is discussed in Basu et al. (1996).

Three sets of helioseismic data have been used for this work. The first set is the data from the Big Bear Solar Observatory (Libbrecht, Woodard and Kaufman, 1990) combined with the low degree ($0 \leq \ell \leq 3$) modes from the Birmingham Solar Oscillation Network (Elsworth et al. 1994), this set is referred to as the BBSO set. The second set consists of the frequencies obtained from the average spectra of months 4 – 14 obtained by the Global Oscillation Network Group (hereafter referred to as the GONG data), and the third set are the frequencies from the data obtained by the SOI/MDI instrument on board the SOHO spacecraft during its first 144 days in operation (Rhodes et al. 1997), which we shall refer to as the MDI data. We restrict ourselves to the frequency range of 1 to 3.5 mHz. The BBSO set is further restricted to a degree range of $\ell \leq 140$ to avoid frequencies determined by the ridge fitting method which may have large systematic errors.

We have used two reference models with identical physical inputs, but different radii for the inversions. Both models

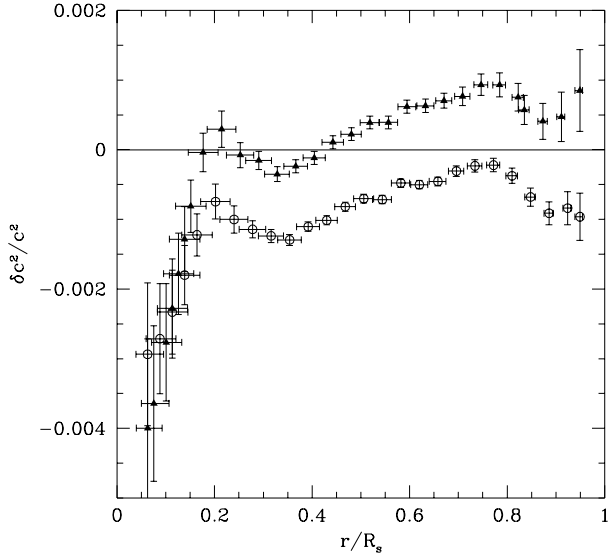


Fig. 2 The relative sound-speed difference between the Sun and two reference models R99 and R78 at fixed fractional radius. The differences are in the sense (Sun – model)/model. The triangles are the results obtained with a reference model of R99 (radius 695.99 Mm), the circles are obtained with reference model R78 (radius 695.78 Mm). The vertical error bars show the 1σ error in the inversions due to errors in the data. The horizontal error-bars are a measure of the resolution. The sound-speed difference between the two models can be seen in Fig. 1(b).

are static-models, constructed with the OPAL equation of state (Rogers, Swenson & Iglesias 1996) and OPAL opacities (Iglesias & Rogers 1996) which are supplemented by the low temperature opacities of Kurucz (1991). The CM formulation is used to calculate the convective flux. To construct the model we use the helioseismically determined hydrogen abundance profile from Antia & Chitre (1997a), and also use the heavy elements abundance profile adopted by them. The surface ratio of heavy elements to hydrogen abundance was constrained to be 0.0245, the value determined from observations by Grevesse & Noels (1993). The radii used are the standard value of 695.99 Mm (Model R99) and the reduced value 695.78 Mm (Model R78) as determined by Antia (1997). In this paper we denote the radius of the solar models as R_s , to avoid confusion with R_\odot , which is normally assumed to have the fixed value of 695.99 Mm.

The sound-speed difference between the Sun and the two models are shown in Fig. 2. The sound-speed difference between the two models has been shown earlier in Fig. 1(b), and hence it is easy to see that there is a real difference between solar sound-speed deduced by using the two models. The same is true for solar density. To make comparisons easier, we have represented the calculated sound-speed profiles as differences with respect to the Model S of Christensen-Dalsgaard et al. (1996) in Fig. 3(a).

Thus it can be seen that there is a significant difference between the results obtained using the two models, which arises because of the difference in radius. In fact, for sound-speed, the relative difference between the two solutions is of the same order as the relative sound-speed difference between the Sun and the two reference models. Thus it is important to invert solar oscillation frequencies using reference

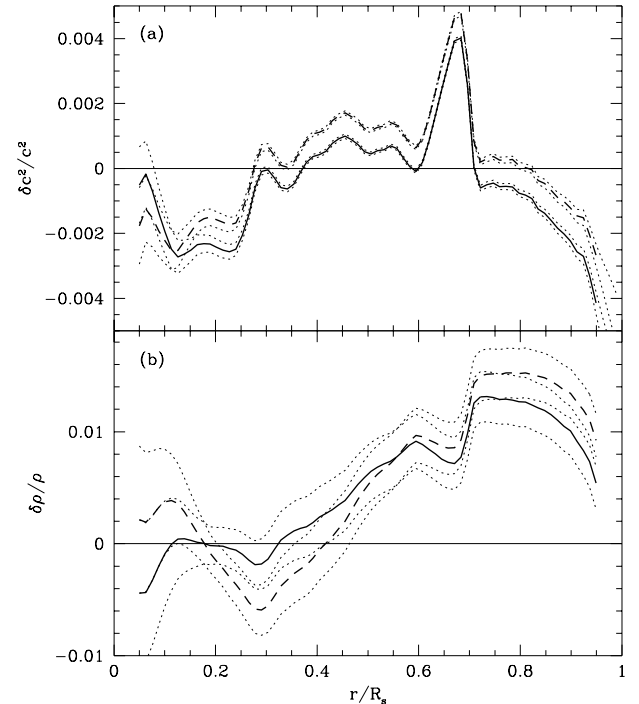


Fig. 3 (a) The sound-speed and (b) density inside the Sun as obtained by the two reference models R99 and R78 shown with respect to Model S of Christensen-Dalsgaard et al. (1996). In both panels, the continuous line represents the result obtained with model R78 ($R_s = 695.78$ Mm) and the dashed line that that obtained using model R99 ($R_s = 695.99$ Mm). The dotted lines represent the 1σ error envelope.

models with the same radius as the Sun. Fig. 3(b) shows the density results obtained using the two models. Again there is a real difference in the result obtained, though in the case of density, the changes are within the 1σ error limits.

The sound-speed difference near the surface between Model S and the Sun shows a very sharp dip which may be attributed to the difference in radius. In fact, the sound-speed difference at fixed radius between models R99 and R78 shows a sharp decrease at the surface, which may lead one to assume that the change in the radius of the reference model will reduce the dip. However, this decrease is not very evident in differences taken at fixed fractional radius (cf., Fig. 1b), which is what is used in the inversions, and hence it is unlikely to affect the inversion results significantly. In fact, we can see from Figs. 2 and 3 that the surface behaviour of the solutions is not very different regardless of the radius of the model used for inverting the solar oscillation frequencies. Thus we believe that the sharp decline in the relative sound-speed difference is more a result of the other physical properties of the model.

To confirm this point we have constructed reference solar models using physical inputs which give rise to large changes in the surface layers as compared to the two reference models used above. One set consists of models with the two different radii and constructed using the mixing length theory (MLT) for calculating the convective flux instead of CM formulation. The models are called MLT99 (for $R_s = 695.99$ Mm) and MLT78 (for $R_s = 695.78$ Mm). We also have one low radius model where instead of Kurucz

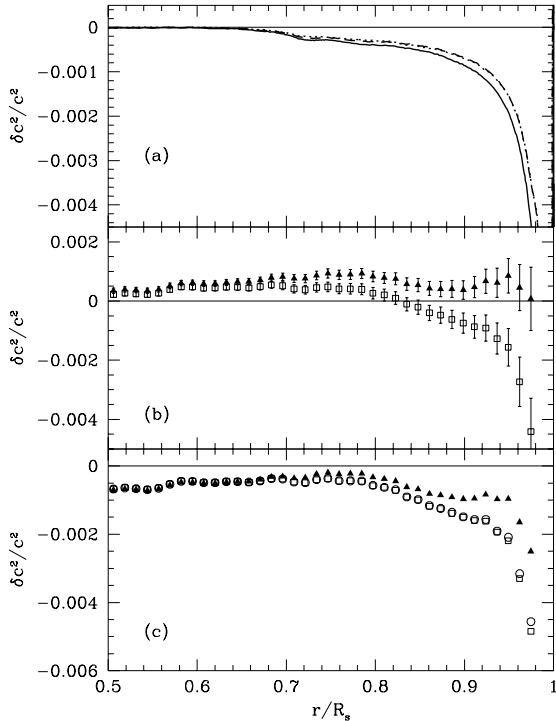


Fig. 4 (a) The relative sound-speed difference between the reference models R99 and R78 and the models with modified physics. The differences are calculated in the sense (reference – modified). The continuous line is the difference between models R78 and OP78, the dotted line is the difference between models R99 and MLT99 and the dashed line is the difference between models R78 and MLT78. Note that the dotted and dashed lines more or less coincide. (b) The relative sound-speed difference between the Sun and model R99 (triangles) and MLT99 (squares). (c) The relative sound-speed difference between the Sun and models R78 (triangles), MLT78 (squares) and OP78 (circles). The error-bars are omitted in this panel for the sake of clarity.

opacities, the OPAL opacities as used as far as the table continue. Below that opacities from Alexander (1975) are used. However, in that region the temperature stratification is obtained using the $T - \tau$ relation of Vernazza et al. (1981). This model is called OP78.

The relative difference in sound-speed between our original reference models and the modified models are shown in Fig. 4(a). Note that the modified models have a higher sound speed in the surface layers as compared to the models with the CM formulation of convection and Kurucz opacities, thus the sound-speed difference between the Sun and the modified models is likely to show a dip at the surface. The results of the inversion are shown in Fig. 4 (b) and (c). The new models, irrespective of radius, do show a sharp decrease in the sound-speed difference in the surface layers. Thus it is clear that a difference in radius is not the cause of the near-surface plunge in the relative sound-speed difference seen between the Sun and Model S.

Fig. 4 also supports the result of Basu & Antia (1994a) that the models constructed with the CM formulation are closer to the Sun than those with MLT formulation. It also appears that the Kurucz (1991) opacities fit solar data better than just the OPAL opacities supplemented by those from Alexander (1975). This appears to support the results of

Antia & Basu (1997) using just the frequency differences. However, there remains a small dip near the surface which points to remaining deficiencies in model R78.

The change in the deduced solar sound-speed profiles because of changes in the radius necessitates the re-calibration of quantities derived from the sound-speed difference. We therefore, look next at the depth and helium abundance of the solar convection zone.

3 DEPTH OF THE CONVECTION ZONE

The transition of the temperature gradient from the adiabatic to radiative values at the base of the solar convection zone (CZ) leaves its signature on the sound speed. Thus helioseismic measurements of the sound speed enables a determination of the position of the base of the convection zone (cf., Christensen-Dalsgaard, Gough & Thompson 1991; Kosovichev & Fedorova 1991; Guzik & Cox 1993; Basu & Antia 1997).

3.1 The Procedure

We use the technique described in Basu & Antia (1997) to determine the position of the CZ base, r_b . To recapitulate briefly, if there are two otherwise similar solar models with different depths of the convection zone, then just below the base of the convection zone the model with a deeper convection zone will have a larger sound speed than the other. This observable difference of sound speeds can be calibrated to find the convection-zone depth of a test model or the Sun.

Asymptotically, the frequency differences between a solar model and the Sun, or between two solar models can be written as (Christensen-Dalsgaard, Gough & Thompson 1989)

$$S(w) \frac{\delta\omega}{\omega} = H_1(w) + H_2(w), \quad (2)$$

where $w = \omega/(\ell + 0.5)$, and $S(w)$ is a known function for a given reference model. The functions $H_1(w)$ and $H_2(w)$ can be found by a least-squares fit to the known frequency differences. $H_1(w)$ can be inverted to obtain the sound-speed difference, $\delta c/c$, between the reference model and the Sun. However, that is not required as $H_1(w)$ itself can be used to determine the convection-zone depth.

If $\phi(w)$ is the $H_1(w)$ between two solar models which differ only in the depth of the convection zone, then $H_1(w)$ for any other pair of models can be written as

$$H_1(w) = \beta\phi(w) + H_s(w), \quad (3)$$

where $H_s(w)$ is a smooth component of $H_1(w)$ which results from sound-speed differences that arise from differences in the equation of state, abundances, surface physics etc., and the first term is the contribution to $H_1(w)$ due to the sound-speed difference caused by the difference in r_b , the position of the base of the CZ. Thus if β is determined by a least squares fit, the unknown r_b of the Sun can be obtained.

We determine β for a series of calibration models with different r_b , and interpolate to find the position for which $\beta = 0$. The error in the CZ depth arising from those in the observed frequencies is determined by Monte Carlo simulations.

As is clear from the above discussion, we need to use models with a specified depth of CZ. This is easier with models of the solar envelope, where position of the CZ base and the helium abundance of the solar envelope can be specified. As Basu & Antia (1997) have shown, the largest source of systematic error in the results is the hydrogen abundance profile. This is because the sound speed near the base of the CZ is affected not only by the change in the temperature gradient, but also by the change in the mean molecular weight due to gravitational settling of helium. Since the X and Z profiles are not known exactly, we use models with three types of profiles:

ND: The hydrogen and heavy element abundance profiles from the no-diffusion model of Bahcall & Pinsonneault (1992).

DIF: The hydrogen abundance profile from solar model of Bahcall & Pinsonneault (1992) incorporating the diffusion of helium and Z profile from Proffitt (1994).

INV: The hydrogen abundance profile obtained from helioseismic inversions (Antia & Chitre 1997a) and the Z profile adopted in that paper.

For each type of model, we have two sets of calibration models, one with the standard radius of 695.99 Mm and the other with the reduced radius of 695.78 Mm. Each calibration set consists of 5 models with CZ-base positions at 0.709, 0.711, 0.713, 0.715 and 0.717 R_s . Thus we have 6 sets of calibration models. In addition, we have test models for each hydrogen abundance profile and each radius, with $r_b = 0.712 R_s$. We also have test models with an even lower radius of 695.57 Mm, to check for trends. For convenience, the models are referred to by their radius (99 for 695.99 Mm, 78 for 695.78 Mm and 57 for 695.57 Mm), hydrogen and heavy element abundance profile and radius of the CZ base, e.g., DIF99-0.709 is the model with the DIF X and Z profiles, with $r_b = 0.709 R_s$ and standard radius ($R_s = 695.99$ Mm), INV78-0.711 is the model with INV X profile, $r_b = 0.711 R_s$ and smaller radius ($R_s = 695.78$ Mm), etc. All models have been constructed with the OPAL equation of state, OPAL and Kurucz opacities and with the CM formulation for calculating convective flux. They have identical surface X of 0.7342 and surface (Z/X) of 0.0245. The systematic errors arising due to variations in these parameters were studied by Basu and Antia (1997).

3.2 Results

The results for the test models are listed in Table 1. We have shown the results for the INV models only. The results for the other calibration models are similar. We can see that there is indeed some difference in the measured value of radial position of the CZ base, when reference models with a different radius are used. The difference is of the order of the relative difference in the radius, but is somewhat smaller than error in the sound speed caused by mismatch of radius. The reason for this can be seen in Fig. 5, where we have shown the function $H_1(w)$ for model INV78-0.712 and the INV99 and INV78 calibration models. $H_1(w)$ is flat in the CZ for INV78 calibration models. This is consistent with the convection-zone sound-speed difference between these models and the test model INV78-0.712 being 0. The predominant difference between the results with INV99 and INV78 models is a linear shift. The truly linear part of the

Table 1. CZ results for the test models

Test model	Deduced r_b/R_s	
	$R_s = 695.99\text{Mm}$	$R_s = 695.78\text{Mm}$
	Calib. models with INV X profile	
INV99-0.712	0.712000	0.712258
INV78-0.712	0.711746	0.712000
INV57-0.712	0.711498	0.711746

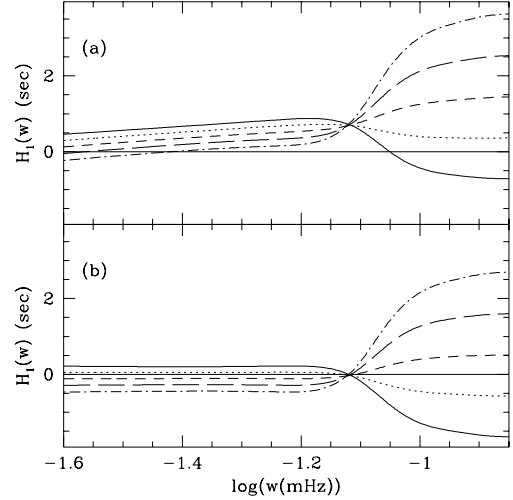


Fig. 5 The function $H_1(w)$ between the model INV78-0.712 and (a) the INV99 calibration models and (b) the INV78 calibration models. In both panels, the continuous line shows $H_1(w)$ between the test model and the calibration model with $r_b = 0.709 R_s$, the dotted line is with $r_b = 0.711 R_s$, small-dashed line with $r_b = 0.713 R_s$, long-dashed line with $r_b = 0.715 R_s$ and dot-dashed line with $r_b = 0.717 R_s$.

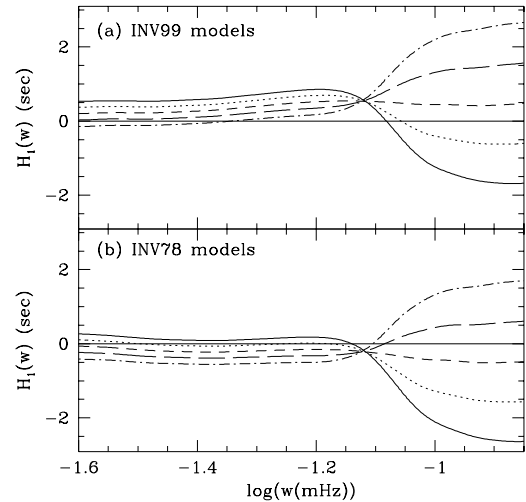


Fig. 6 The function $H_1(w)$ between the Sun and (a) the INV99 calibration models and (b) the INV78 calibration models. The line types are the same as in Fig. 5.

shift is easily removed by the function $H_s(w)$ in the fit to Eq. (3), hence the r_b results for this model are not very different. Nevertheless, the error arising due to difference in radius is larger than the error in the solar results because of errors in the frequencies, and hence the solar CZ depth should be determined using the models with the correct radius. The difference in r_b due to a difference in the radius is

Table 2. CZ results for the Sun

Data set	Deduced r_b/R_s		
	ND78 models	INV78 models	DIF78 models
BBSO	0.714219 ± 0.000179	0.713435 ± 0.000175	0.710665 ± 0.000181
GONG	0.714149 ± 0.000062	0.713430 ± 0.000060	0.710631 ± 0.000062
MDI	0.714443 ± 0.000080	0.713601 ± 0.000078	0.710868 ± 0.000081
Weighted Average	0.714267 ± 0.000050	0.713494 ± 0.000049	0.710722 ± 0.000051

much smaller than that due to differences in the hydrogen abundance profile. For example, the error in determining the position of the CZ base can be as much as $0.0035 R_s$ (cf., Basu & Antia 1997) between the DIF and ND profiles.

The function $H_1(w)$ between the Sun and the two sets of INV calibration models are shown in Fig. 6. Note that $H_1(w)$ for models with $R_s = 695.78$ Mm is much flatter in the CZ as compared to models with $R_s = 695.99$ Mm. This gives added confidence that the solar radius is indeed close to 695.78 Mm. Table 2 lists the position of the solar CZ base as obtained using different data sets and different calibration models.

Since it can be shown that models with the DIF profile have too sharp a gradient in the X -profile at the CZ base (Basu 1997a), we can disregard the value obtained with those models. There is an enormous amount of evidence that diffusion of helium and heavy elements does take place below the solar CZ base (see e.g. Basu 1997b), the value obtained with the ND models is thus an upper limit to the value of r_b , as models with diffusion will give lower values. The value obtained with the INV models is probably the most reliable determination. The change in the results is negligible if instead of the INV profiles, those obtained from stellar evolution codes that incorporate mixing due to rotation (e.g., Richard et al. 1996) are used.

The various other systematic errors that can creep into the determination of the position of the CZ base have been discussed in detail in Basu & Antia (1997). They are invariably larger than the statistical error due to the error in frequencies. This gives an error of $0.0005R_s$, which is larger than the error due to the uncertainty in the radius.

The base of the convection zone is therefore estimated to be at $0.7135 \pm 0.0005R_s$. If models with the standard radius are used, we find a position of $0.7132 \pm 0.0005R_s$ using the same data sets.

3.3 CZ depth and Z/X from density differences

The sound speed inside the convection zone is not particularly sensitive to the composition or the position of the convection-zone base. The difference in the sound speed between various models occurs below the CZ base. Thus it is difficult to disentangle the change in sound-speed below the CZ base because of change in temperature gradient from that due to changes in the mean-molecular weight due to gravitational settling of helium and heavy elements. This is the reason that the models with different composition profiles give seemingly different estimates of the position of the CZ base. The density in the CZ is, however, affected by the position of the CZ base, which arises because of difference in mixing length required to achieve different depths of CZ.

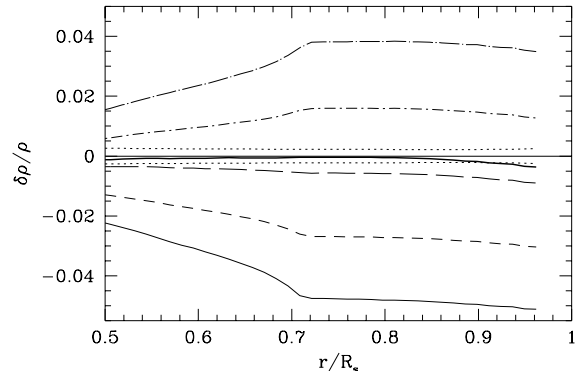


Fig. 7 The relative density difference between the Sun and the INV78 calibration models. The thin-continuous, small-dashed, long-dashed, dot-small dashed and dot-long dashed lines are the differences for the models with $r_b = 0.709, 0.711, 0.713, 0.715$ and $0.717 R_s$ respectively. The thick continuous line is for the model with the CZ base at the position estimated using the above calibration models ($r_b = 0.7135R_s$). The dotted lines show the 1σ error in the density inversion.

This can be seen from Fig. 7, where we show the density difference between Sun and the INV calibration models. We have also shown the density difference for the model with the CZ base at the deduced position of $0.7135R_s$. Note that the density difference for this model is consistent with 0, which gives us added confidence in the results. It may be noted that the position of the base of the convection zone is determined by the opacity and in principle, it is possible to estimate the opacity at the CZ base by using the inversion results coupled with an estimate of the position of the CZ base. Analyses using density differences unfortunately suffer from the drawback that density in the CZ is also dependent on the low-temperature opacities used and to some extent on the composition within the CZ.

As can be seen from Fig. 7, the density difference between the INV78 model with $r_b = 0.7135$ and surface $Z/X = 0.0245$ and the Sun is almost zero. This would mean that assuming that r_b and Z/X are correct, the opacities used in the model, i.e., OPAL supplemented by Kurucz, are consistent with helioseismic data. The uncertainty in the estimated depth of the CZ base i.e., $0.0005R_s$ corresponds to a change of opacity at the CZ base by 0.6%, which is much smaller than the probable uncertainties in the opacity. The largest change in opacity occurs when Z/X is changed. If Z/X is changed by the quoted uncertainty of 10%, the opacities also show almost 10% change. Thus we can conclude that with the current values of Z/X the OPAL opacity tables are consistent with the estimated opacity at the base of the solar CZ.

The good agreement between the estimated opacity and that calculated from the OPAL tables using the currently accepted value of Z/X suggests that the uncertainty in Z/X should be much smaller than the quoted error of 10%. Assuming the correctness of the OPAL opacities we can use the CZ-density differences between the Sun and the models to put limits on the amount of heavy elements in the solar envelope. The solar models constructed with $r_b = 0.7135R_s$, $Y = 0.2478$ and $Z/X = 0.0245$ shows a near perfect fit to the CZ density. If we keep Y the same, then we find that a change in Z/X of ± 0.0001 changes the density difference by $\pm 1\sigma$. If we keep X fixed and change Z/X then a change of ± 0.0002 changes density by $\pm 1\sigma$. In addition there are uncertainties caused by errors in the depth of the CZ, the low temperature opacities, the hydrogen abundance in the CZ, and uncertainties in the solar-radius. Taking into account all these uncertainties we estimate that the heavy element abundance in the solar envelope is $Z/X = 0.0245 \pm 0.0006$, i.e., the uncertainty is much less than the normally assumed uncertainty of 10% in spectroscopically estimated value.

3.4 Overshoot below the solar CZ base

Solar oscillation frequencies can be used to determine the extent of overshoot below the solar convection zone if it is assumed that the overshoot region is adiabatically stratified and that there is an abrupt transition to radiative stratification below the overshoot zone. This change in stratification introduces a discontinuity in the first derivative of the sound-speed and leaves a characteristic oscillatory signal in the frequencies. The amplitude of the signal can be calibrated to determine the extent of overshoot (cf., Monteiro, Christensen-Dalsgaard & Thompson 1994; Basu & Antia 1994b; Basu 1997a). Basu (1997a) had found an upper limit of $0.05H_p$ on the overshoot region. That was done using models with the standard radius of 695.99 Mm. We have tried to see whether models with the lower radius show a change in the amplitude of the signal and whether the use of the new data changes the limits. The procedure used for fitting is described in Basu (1997a).

We constructed a few models to test the change of the amplitude with radius and extent of overshoot. All models are INV models. The CZ depth of the models is appropriate for the radius of the model. The results for the different models and data sets are shown in Table 3. The addition of the two data sets does not change the observed results significantly. The change in the amplitude of the signal with change in radius is smaller than the statistical error in the amplitude due to uncertainties in observed frequencies. Hence the conclusions about the extent of overshoot below the solar convection zone are not affected by possible error in solar radius.

4 HELIUM ABUNDANCE

Spectroscopic measurements of the abundance of helium in the Sun being very uncertain, helioseismology plays a major role in determining the helium abundance in the solar envelope. The abundance is obtained from the variation of the adiabatic index of the solar material in the helium ionisation zone, which in turn affects the sound speed.

Table 3. Amplitude of signal form CZ base

Model	Amplitude (μHz)	
	INV99	INV78
Ov.=0 H_p	0.8020	0.8073
Ov.=0.05 H_p	0.9014	0.9071
Ov.=0.10 H_p	1.0428	1.0494
Observations		
BBSO	0.879 ± 0.106	
GONG4-14	0.782 ± 0.032	
MDI	0.771 ± 0.034	
Weighted Average	0.790 ± 0.025	

4.1 The procedure

The technique used here is the same as that in Antia & Basu (1994b) and Basu & Antia (1995), and is very similar to that used to determine the depth of the CZ zone. The starting point of the procedure is again Eq. (2). However, since the data do not extend to high degrees and the data sets have hardly any modes with turning points in the helium ionisation zone ($r > 0.98R_s$), it is difficult to use $H_1(\omega)$ to determine the helium abundance. We have to use the function $H_2(\omega)$ instead. It has been shown that (e.g., Basu & Antia 1995; Pérez Hernandez & Christensen-Dalsgaard 1994), the helium ionisation zone being sufficiently close to the solar surface leaves its imprint on the function $H_2(\omega)$ also, in the form of a hump around 2.5 mHz, which can be calibrated to determine the helium abundance. The effect of difference in other physical properties, like the equation of state, manifests itself as a smooth curve on which the hump due to difference in helium abundance is superimposed.

Thus, analogous to Eq. (3), we write the function $H_2(\omega)$ between the Sun and a calibration model of known helium abundance as:

$$H_2(\omega) = \beta\Phi(\omega) + H_s(\omega), \quad (4)$$

where $\Phi(\omega)$ is the difference in $H_2(\omega)$ between two models which differ only in the abundance of helium.

For this work too it is preferable to use envelope models since the calibration models are required to have specified values of the helium abundance. Since by far the largest error in helium abundance determination occurs due to a mismatch of the equation of state (cf., Antia & Basu 1994b), we use models with both OPAL and the MHD (Hummer & Mihalas 1988; Mihalas, Däppen & Hummer 1988; Däppen et al. 1988) equations of state. For each equation of state, we have constructed calibration sets with radii 695.99 Mm and 695.78 Mm. Each calibration set consists of five models with hydrogen abundance X of 0.68, 0.70, 0.72, 0.74 and 0.76. The value of the metal abundance Z was kept fixed at 0.018 for the OPAL models. For the MHD models, the available tables force $Z = 0.02$. All models have the CZ base at $r_b = 0.713 R_s$. In addition, we have test models with $X = 0.73$ for both equations of state and both values of the radius. We also have constructed test models with $R_s = 695.57$ Mm. The models are labelled by their EOS (OPAL or MHD), radius (99 for 695.99 Mm, 78 for 695.78 Mm and 57 for 695.57 Mm), and surface hydrogen abundance. Since the helium ionisation zone is very far from the CZ base, it is not expected to be affected by the abundance profiles below

Table 4. Helium abundance results for the test models

Test model	Exact Y	Deduced Y	
		$R_s = 695.99$ Mm	$R_s = 695.78$ Mm
Calib. models with OPAL EOS			
OPAL99-0.73	0.252	0.25184	0.25156
OPAL78-0.73	0.252	0.25212	0.25184
OPAL57-0.73	0.252	0.25240	0.25212
MHD78-0.73	0.250	0.24938	0.24904
Calib. models with MHD EOS			
MHD99-0.73	0.250	0.24987	0.24957
MHD78-0.73	0.250	0.25016	0.24987
MHD57-0.73	0.250	0.25046	0.25016
OPAL78-0.73	0.252	0.25373	0.25355

Table 5. Helium abundance results for the Sun

Data set	Deduced Y	
	$R_s = 695.99$ Mm	$R_s = 695.78$ Mm
OPAL models		
BBSO	0.2476 ± 0.0002	0.2474 ± 0.0002
GONG	0.2471 ± 0.0001	0.2470 ± 0.0001
MDI	0.2488 ± 0.0001	0.2488 ± 0.0001
MHD models		
BBSO	0.2514 ± 0.0002	0.2510 ± 0.0002
GONG	0.2499 ± 0.0001	0.2496 ± 0.0001
MDI	0.2524 ± 0.0001	0.2522 ± 0.0001

the CZ base. Hence, the models constructed for calibrating the helium abundance do not assume any diffusion of helium or heavy elements below the CZ base.

4.2 Results

The value of Y obtained for different models are listed in Table 4. Note that unlike the case of the CZ depth, where the CZ depth of the models with same R_s could be determined accurately, there is an error of about 0.0002 in the determination of the helium abundance even when the radius is the same. The main reason is that the signature due to differences in helium abundance is not as clear-cut as that due to differences in the position of the CZ base. Another reason for this is that the mode-sets used do not have modes with turning points in the helium ionisation zone. Nonetheless, we see that there is an additional error if the radius of the calibration and test models differs. The magnitude of the difference is of the order of the fitting errors in the determination of helium abundance. However, as we shall show below, there are larger errors caused by a number of other factors, such as opacity used etc. Hence the solar results are unlikely to be affected significantly by a change in radius of the calibration models.

Since the contribution to $H_2(\omega)$ at any given frequency comes from modes with different turning points, the deduced helium abundance may be affected by model differences not necessarily localised at the helium ionisation zone. To test this we have constructed a few additional models to test the error in the deduced helium abundance caused because of differences in composition profile below the CZ base, depth of CZ and opacities used. As expected, the composition profile below the CZ base does not affect the determination of He abundance. However, the depth of the CZ does. An error

of $0.0005R_s$ in the CZ depth causes an error of 0.0003 in Y . A much larger error of 0.0006 is produced if the low temperature Kurucz (1991) opacities are replaced by those of Alexander (1975). We estimate that the uncertainty in the deduced helium abundance due to all these factors is about 0.001.

The results for the Sun are listed in Table 5. The error-estimate corresponds merely to the error in the result due to those in the frequencies, and as can be seen in light of the discussion above, are much smaller than the systematic errors involved. Unlike in the case of CZ depth determination, the different data sets give results that are not consistent with each other within the errors. We believe this is a result of the different degree ranges of the three data sets. For a definitive determination of the helium abundance, one needs high-degree p-modes which have lower turning points in the helium ionisation zones. None of the data-sets used has such high degree modes. The highest-degree p-mode in the MDI set has $\ell = 194$, in the GONG set it has $\ell = 150$ and the BBSO set has been deliberately restricted to modes of $\ell \leq 140$ to avoid using modes with large systematic errors. Since none of the mode-sets has modes which sample the helium ionisation zone very well, it is not very surprising that the results with the three data sets are different

As expected (cf., Basu & Antia 1995; Kosovichev 1996; Baturin & Ayukov 1997), MHD and OPAL models give different results for the Sun. The result obtained for the OPAL models, an average of the three sets being $Y = 0.2478$, is not very different from the earlier result of $Y = 0.249$ obtained by Basu & Antia (1995), and are the same as those of Kosovichev (1996). The current results are, however, expected to be more reliable since the radius of the models is consistent with that of the Sun and the data-sets used are better. For models with the standard radius of 695.99 Mm, we find $Y = 0.2479$, with an uncertainty of 0.001 in the results due to fitting errors and systematic error mentioned above.

The result for the MHD models on the other hand is somewhat higher than that obtained by Basu & Antia (1995) but are consistent with those of Baturin & Ayukov (1997). The results obtained by different workers using MHD models have a wide dispersion. This may be due to the fact that the sound-speed difference between all MHD models and the Sun show a distinct deviation just below the helium ionisation zone (cf., Dziembowski, Pamyatnykh & Sienkiewicz 1992; Basu & Antia 1995), which can contaminate the signal from the helium abundance to varying degrees depending on the procedure followed to estimate the helium abundance in the solar envelope.

5 THE SOUND-SPEED DIFFERENCE IN THE CZ

Fig. 8 shows the sound-speed difference between the Sun and four solar models in the convection zone. There are two OPAL models and two with the MHD EOS. For each EOS, one model has the standard radius of 695.99 Mm and one the reduced radius of 695.78 Mm. Each model has a CZ-base position and helium abundance appropriate to its radius and EOS (cf., Sections 3 and 4). Note that the sound-speed of the Sun is higher than that of the two models with the standard radius. For the reduced-radius models, the solar sound-speed is higher than the sound-speed of the

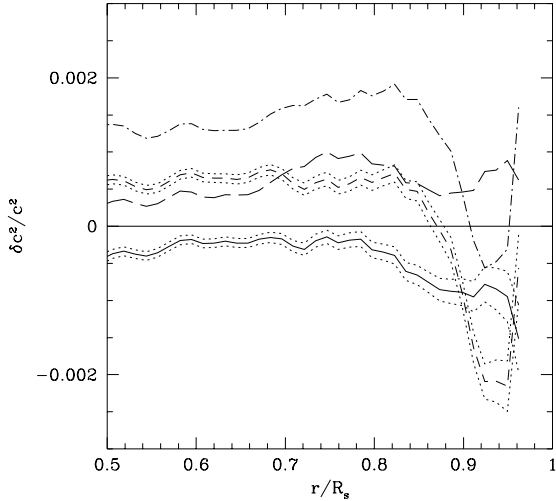


Fig. 8 The relative sound-speed difference between solar envelope models and the Sun. The continuous line and the small-dashed line are for models with $R_s = 695.78$ Mm, constructed with OPAL and MHD equations of state respectively. The dotted lines are the 1σ error envelope. The long-dashed and the dot-dashed lines are for models with $R_s = 695.99$ Mm, constructed with OPAL and MHD equations of state respectively. For the sake of clarity, the error envelopes have not been shown for these models.

MHD model, but is marginally lower than that of the OPAL model. The overall difference is however much lower than the models with the standard radius.

There are a number of possibilities as to why the sound-speed in the lower part of the CZ in the models do not match that of the Sun, these are, for instance, that the change in radius has not been estimated correctly or that the equation of state is not correct.

Looking at Fig. 8, it appears that the change in radius has over-corrected the sound-speed in the case of the OPAL model, while the correction is not enough for the MHD models. Thus, for the OPAL models the reduction of radius to 695.78 Mm is an overestimate of the reduction, while for the MHD models it is an underestimate. The radii at which the models show very little difference with respect to the solar sound speed in the lower CZ are 695.82 Mm and 695.67 Mm respectively for the OPAL and MHD EOS. This additional change in radius, however, causes the f-mode frequencies of the model to deviate from the observed frequencies. This means that either the surface layers of the solar models have not been modelled properly, or other processes, like flows etc., may need to be postulated to explain the f-mode frequency difference.

The structure of lower part of the solar convection zone is determined mainly by the equation of state, hence an error in the equation of state will give rise to a sound-speed difference between a solar model and the Sun. Thus if we assume that the radius and helium abundance in CZ have been estimated correctly, the remaining discrepancy in the sound speed may be due to possible error in the equation of state. It is clear from Fig. 9 that the OPAL EOS is much closer to that of the solar material than the MHD EOS. However, there is still some remaining difference. We find that for the reduced radius models, a large part of the difference can be eliminated if the partial derivative $(\partial p/\partial T)_\rho$ for the OPAL equation of state is lowered by a factor $(1 - 0.00027)$,

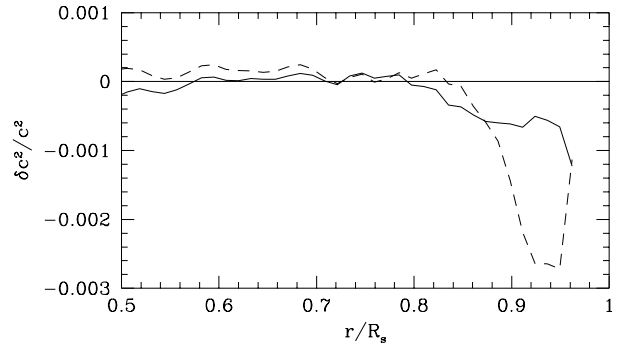


Fig. 9 The relative sound-speed difference between solar envelope models and the Sun. Both models have a radius of 695.78 Mm. The continuous line is for a model constructed with a modified OPAL EOS, and the dashed line is for a model constructed with modified MHD EOS.

and the other thermodynamic quantities like C_p and Γ_1 are changed consistently. This corresponds to a relative difference of about -0.00022 in Γ_1 between the two models in the lower part of the CZ. For the MHD EOS, the partial-derivative should be larger by a factor 1.00053, this results in a relative difference of 0.00043 in Γ_1 . This small difference largely eliminates the sound-speed difference in the CZ, as can be seen from Fig. 9. It is not obvious that the discrepancy is indeed due to an error in equation of state, but these differences probably give an estimate of uncertainties in current equations of state. This change in EOS does not change the f-mode frequencies significantly.

6 CONCLUSIONS

We have shown that a mismatch in the radius of the Sun and that of reference solar models can introduce considerable error in the inverted sound-speed and density profiles of the Sun. The relative difference in the sound speed obtained by inversion due to the change in radius is of the same order as the relative difference between the sound speed of the Sun and the solar models used. Therefore, inversion of solar oscillation frequencies to determine solar structure should be performed using models with radius as close as possible to the correct value. Thus it is necessary to obtain an accurate estimate of the solar radius.

We find that regardless of the radius of the solar models used, solar models constructed using the CM formulation of convection give a better fit to the near-surface solar sound speed than models constructed with the mixing length formalism. Models constructed with the mixing length formalism show a sharp dip in the relative sound-speed difference with respect to the Sun in the outer regions, and this dip is not removed by the reducing the radius of the solar models.

We have used new data-sets to check how the change in radius results in a small change in the measured depth of the solar convection zone and in the helium abundance. We obtain a radial distance of $(0.7135 \pm 0.0005)R_s$ for the base of the CZ. We also find that the OPAL tables are consistent with the solar opacities at the CZ base for a surface Z/X of 0.0245. Assuming that the OPAL opacities are correct, we deduce that the the surface $Z/X = 0.0245 \pm 0.0006$ with an error estimate which is much less than the usually quoted value of 10%. The limit on the extent of overshoot does not

change because of the small change in radius, and remains at $0.05H_p$ (2800 Km).

Using the new data sets and models constructed with the OPAL equation of state, we find that the helium abundance in the solar envelope is 0.2478 ± 0.001 . Once again, the estimate of helium abundance is not significantly affected by the error in radius as the effect is smaller than the systematic errors in this measurement.

If the correct R_s is indeed 695.78 Mm and abundances in CZ have been estimated correctly, then the remaining discrepancies between the CZ sound-speed profile of the models and the Sun can be explained as errors in the equation of state used. It can be shown that by changing $(\partial p/\partial T)_\rho$ for each EOS suitably, one can reduce the difference. For OPAL models this has to be reduced by a factor of 0.99973, while for MHD models this has to be increased by a factor 1.00053. Changes in $(\partial p/\partial T)_\rho$ automatically changes the adiabatic index Γ_1 , and corresponds to a decrease in Γ_1 by a factor of 0.99978 for OPAL models and an increase by a factor of 1.00043 for MHD models. This probably gives an estimate of uncertainties in the current equations of state.

ACKNOWLEDGMENTS

This work utilizes data obtained by the Global Oscillation Network Group (GONG) project, managed by the National Solar Observatory, a Division of the National Optical Astronomy Observatories, which is operated by AURA, Inc. under a cooperative agreement with the National Science Foundation. The data were acquired by instruments operated by the Big Bear Solar Observatory, High Altitude Observatory, Learmonth Solar Observatory, Udaipur Solar Observatory, Instituto de Astrofísica de Canarias, and Cerro Tololo Inter-American Observatory. SOHO is a project of international cooperation between ESA and NASA. The author was supported by an AMIAS fellowship and the Institute for Advanced Study SNS Membership fund.

REFERENCES

- Alexander D. R., 1975, *ApJS*, 29, 363
 Antia H. M., 1997, *A&A*, in press (astro-ph/9707226)
 Antia H. M., Basu S., 1994a, *A&AS*, 107, 421
 Antia H. M., Basu S., 1994b, *ApJ*, 426, 801
 Antia H. M., Basu S., 1997, in eds. Pijpers F. P., Christensen-Dalsgaard J., Rosenthal C., *Solar Convection and their Relationship*, (Dordrecht: Kluwer), p51
 Antia H. M., Chitre S. M., 1997a (astro-ph/9710159)
 Antia H. M., Chitre S. M., 1997b, in Proc: IAU Symp. 185, in press
 Allen C. W. 1976, *Astrophysical Quantities* (3d ed.; London: Athlone)
 Bahcall, J. N., & Pinsonneault, M. H., 1992, *Rev. Mod. Phys.* 64, 885
 Balmforth N. J., 1992, *MNRAS* 255, 632
 Basu S., 1997a, *MNRAS*, 288, 572
 Basu, S., 1997b, in eds., Provost, J., Schmider, F. -X., IAU Symp. 181: *Sounding Solar and Stellar Interiors*, Kluwer, Dordrecht, in press
 Basu S., Antia H. M., 1994a, *JAA*, 15, 143
 Basu S., Antia H. M., 1994b, *MNRAS*, 269, 1137
 Basu S., Antia H. M., 1995, *MNRAS*, 276, 1402
 Basu S., Antia H. M., 1997, *MNRAS*, 287, 189
 Basu S., Christensen-Dalsgaard J., Schou J., Thompson M. J., Tomczyk S. 1996, *ApJ*, 460, 1064
 Baturin V. A., Ayukov S. V., 1997, in eds. Pijpers F. P., Christensen-Dalsgaard J., Rosenthal C., *Solar Convection and their Relationship*, (Dordrecht: Kluwer), p55
 Canuto, V. M., Mazzitelli, I., 1991, *ApJ* 370, 295
 Christensen-Dalsgaard, J., Gough, D. O. and Thompson, M. J. 1989, *MNRAS* 238, 481
 Christensen-Dalsgaard J., Gough, D. O. & Thompson, M. J. 1991, *ApJ* 378, 413
 Christensen-Dalsgaard J., Däppen W., Ajukov S. V., et al., 1996, *Science*, 272, 1286
 Cox A. N., Kidman R. B., 1986, in *Theoretical Problems in Stellar Stability and Oscillations* (Institut d'Astrophysique, Liège) p259
 Däppen W., Mihalas D., Hummer D. G., Mihalas B. W., 1988, *ApJ*, 332, 261
 Däppen W., Gough D. O., Kosovichev A. G., Thompson M. J., 1991, in eds., Gough D. O., Toomre J., *Lecture Notes in Physics*, 388, Springer, Heidelberg, p.111
 Dziembowski W. A., Pamyatnykh A. A., Sienkiewicz R., 1990, *MNRAS*, 244, 542
 Dziembowski W. A., Pamyatnykh A. A., Sienkiewicz R., 1992, *Acta Astron.*, 42, 5
 Dziembowski W. A., Goode P. R., Pamyatnykh A. A., Sienkiewicz R., 1994, *ApJ*, 432, 417
 Elsworth Y., Howe R., Isaak G. R., et al., 1994, *ApJ*, 434, 801
 Gough D. O., Kosovichev A. G., Toomre J., et al., 1996, *Science*, 272, 1296
 Grevesse N., Noels A. 1993, eds. Prantzos N., Vangioni-Flam E., & Cassé M., in *Origin and evolution of the Elements*, (Cambridge: Cambridge Univ. Press), p15
 Guzik, J. A., Cox, A. N., 1993, *ApJ* 411, 394
 Hill F., Stark P. B., Stebbins R. T. et al., 1996, *Science*, 272, 1292
 Hummer D. G., Mihalas D., 1988, *ApJ*, 331, 794
 Iglesias, C. A. & Rogers, F. J. 1996, *ApJ* 464, 943
 Kosovichev A. G., 1996, *Bull. Astron. Soc. India*, 24, 355
 Kosovichev, A. G., Fedorova, A. V., 1991, *Sov. Astron.*, 35, 507
 Kosovichev A. G., Schou J., Scherrer P., et al., 1997, *Solar Phys.*, 170, 43
 Kurucz R. L., 1991, in eds., Crivellari L., Hubeny I., Hummer D.G., *NATO ASI Series, Stellar Atmospheres: Beyond Classical Models*. Kluwer, Dordrecht, p.441
 Libbrecht K. G., Woodard M. F., Kaufman J. M., 1990, *ApJS*, 74, 11 29
 Mihalas D., Däppen W., Hummer D. G., 1988, *ApJ*, 331, 815
 Monteiro M. J. P. F. G., Christensen-Dalsgaard J., Thompson M. J., 1994, *A&A*, 283, 247
 Pérez Hernández F., Christensen-Dalsgaard J., 1994, *MNRAS*, 267, 111
 Pijpers F. P., Thompson M. J., 1992, *A&A*, 262, L33
 Proffitt C. R. 1994, *ApJ* 425, 849
 Richard O., Vauclair S., Charbonnel C., Dziembowski W. A., 1996, *A&A*, 312, 1000
 Rhodes E. J., Kosovichev A. G., Schou J., Scherrer P. H., Reiter J., 1997, *Solar Phys.*, 175, No:2 in press
 Rogers, F. J., Swenson, F. J., Iglesias, C. A., 1996, *ApJ* 456, 902
 Schou J., Kosovichev A. G., Goode P. R., Dziembowski W. A., 1997, *ApJ*, 489, L197
 Thompson M. J., Toomre J., Anderson E. R., et al., 1996, *Science*, 272, 1300
 Vernazza J. E., Avrett E. H., Loeser R., 1981, *ApJS*, 45, 635

This paper has been produced using the Royal Astronomical Society/Blackwell Science \TeX macros.